

ARTICLES

Phenyl Ring Dynamics of Enkephalin Molecules and Behavior of Bound Solvents in the Crystalline States by ^2H NMR SpectroscopyMiya Kamihira, Akira Naito,^{*,†} Satoru Tuzi, and Hazime Saitô^{*,‡}

Department of Life Science, Himeji Institute of Technology, Harima Science Garden City, Kamigori, Hyogo 678-1297, Japan

Received: July 29, 1998; In Final Form: December 31, 1998

The phenyl ring dynamics of [$^2\text{H}_5$]Phe⁴-labeled Leu⁵- and Met⁵-enkephalin molecules in crystals grown from four solvents were examined using solid state ^2H NMR spectroscopy. ^2H NMR powder patterns clearly indicated the presence of 180° flip motions about the $\text{C}_\beta\text{--C}_\gamma$ bond axis of the phenyl rings. Frequencies of the 180° flip motions were estimated to be 5.0×10^3 , 3.0×10^4 , and 2.4×10^6 Hz for Leu⁵-enkephalin crystallized from H_2O , methanol/ H_2O , and *N,N*-dimethylformamide (DMF)/ H_2O , respectively and 1.0×10^4 Hz for Met⁵-enkephalin crystallized from ethanol/ H_2O at ambient temperature. The difference of the frequencies for the motion was attributed to the manner of their molecular packing in the crystals as determined by X-ray diffraction. Because the correlation times determined from the ^2H spin–lattice relaxation times (T_1^D values) were much shorter than those of the 180° flip motions, it was shown that the phenyl rings of these four crystals have small-amplitude librations. Therefore, we concluded that the T_1^D values were dominated by the librations, even for the ring deuterium. These motions became slower at lowered temperatures and caused the change of the peak intensities and increased quadrupole splittings which were observed in each ^2H NMR spectra. Isotropic sharp signals due to naturally abundant solvent molecules were observed at the center of the ^2H NMR spectra. The stepwise loss of the signal intensity was interpreted in terms of differential temperatures of freezing of motions of both bound water or organic solvent and the mixed solvent as the temperature was lowered, consistent with the buildup of solvent peaks in the ^{13}C CP-MAS NMR spectra. It is suggested that there are a number of bound mobile solvent molecules in the crystals and the freezing of the solvents causes considerable changes in the conformations and dynamics of enkephalin molecules.

Introduction

Enkephalins are endogeneous morphine-like neuropeptides and have primary structures of Tyr¹-Gly²-Gly³-Phe⁴-Leu⁵ (Leu⁵-enkephalin) and Tyr¹-Gly²-Gly³-Phe⁴-Met⁵ (Met⁵-enkephalin).¹ The first four amino acids are commonly found in the N-terminal region of the opioid peptides that bind to three types of opioid receptors (μ , δ , κ) consisting of seven transmembrane helices.^{2–4} Conformational studies for enkephalins or a number of analogues have been performed by X-ray diffraction or solution NMR studies to understand the structure–function relationships.

Leu⁵- and Met⁵-enkephalin molecules do not take a unique secondary structure in H_2O .^{5–7} In dimethyl sulfoxide (DMSO) solution, Leu⁵-enkephalin forms the type I β -bend structure at the Gly³-Phe⁴ moiety,⁸ whereas Met⁵-enkephalin is in equilibrium between the extended and folded conformations which are stabilized by intramolecular attraction.⁵ In the presence of sodium dodecyl sulfate (SDS), Met⁵-enkephalin forms a type IV β -turn structure stabilized by hydrophobic interactions between the aromatic rings of side chains in Tyr¹ and Phe⁴.⁶ X-ray diffraction studies have revealed the existence of polymorphs depending upon the mother liquor used for crystal

growth, namely, the degree of hydration. Although the backbone conformation of the solid structure is classified into three types such as single β -bend,^{9,10} double β -bend,¹¹ or extended forms,^{12–15} there were a variety of torsion angles of the backbones in the same type of structures. It is currently not well understood which structure is close to an active form or a binding form to the specific receptors.

It has been reported that opioid peptides to be bound to these receptors are required to have a positive charge of amino nitrogen and a phenol group of the tyrosine residue which is capable to form a hydrogen bonding with these receptors.^{2,16–18} The sequence of the first three residues in opioid peptides is called as the *message components* on the message–address concept which was originally described as the recognition elements of peptide hormones.¹⁷ Three types of receptors recognize selectively the specific sequences followed by the Gly³-Phe⁴ moiety of ligand molecules that is proposed as the *address components*. For the address components, the aromatic ring of phenylalanine which can have a π – π contact with the aromatic residues of its receptor side is considered to be required for their activity. It is, therefore, important to characterize the flexibility of these aromatic rings of enkephalin molecules to understand how these peptides are bound to a specific site of their receptors in vivo.

[†] E-mail: naito@sci.himeji-tech.ac.jp. Fax: +81-791-58-0182.

[‡] E-mail: saito@sci.himeji-tech.ac.jp. Fax: +81-791-58-0182.

In our previous paper, we have investigated the structure and dynamics of the backbone and side chains for enkephalin taking a variety of polymorphs by ^{13}C and ^{15}N CP-MAS (cross polarization-magic angle spinning), REDOR (rotational echo double resonance) NMR, and relaxation studies.^{19,20} It has also been shown that these enkephalin molecules in the crystals are highly flexible and sensitive to the state of solvent molecules and that the conformations or dynamics of peptides vary depending on the condition of crystal growth.^{20a} In the freshly prepared crystals, the side chains such as the methyl groups of leucine or methionine undergo rapid rotational motions about the 3-fold axes, and tyrosine and phenylalanine rings have a kind of motion of the same order with the proton decoupling frequency (47–54 kHz).^{20a} In the dried form of the crystals, however, these local motions were substantially reduced.^{19,20a} The extent of the reduced peak intensities by this interference with the proton decoupling frequency was not always the same for the samples examined. In addition, the mode and frequencies of the motion in tyrosine and phenylalanine rings were not determined separately because the broadened carbon signals of the rings obscure the individual resonances.

Solid-state ^2H NMR spectroscopy for deuterium-labeled samples provides detailed information on molecular motion with the frequency range from 10^3 to 10^6 Hz as well as the characteristics of the motion such as a free rotation or a 180° flip motion of the phenyl ring about a symmetry axis.²¹ So far, the molecular dynamics of the phenyl rings of Phe residues in solids has been extensively investigated by ^2H NMR spectroscopy for amino acids, polypeptides, and proteins.^{22–25} As for the enkephalin crystal, it turned out that the tyrosine rings have a 180° flip motion with a frequency of 5×10^4 Hz at room temperature for the $[3,5\text{-}^2\text{H}_2]\text{Tyr}^1$ -labeled Leu-enkephalin crystallized from ethanol by ^2H NMR spectroscopy.²⁶ On the other hand, a fairly slow 180° flip motion of the tyrosine ring of Leu-enkephalin with a frequency of 1.3×10^2 Hz was observed in the dried form of the crystals grown from methanol/ H_2O by 2D-exchange NMR spectroscopy.¹⁹ These observations suggest that the degree of motion depends on the environment of the enkephalin molecules such as crystalline packing and the state of the bound solvents.

In the present study, we have examined the motion of phenylalanine rings of $[2,3,4,5,6\text{-}^2\text{H}_5]\text{Phe}^4$ -labeled Leu⁵- and Met⁵-enkephalins in the crystals grown from several kinds of solvents utilizing solid state ^2H NMR spectroscopy. The present results are consistent with the previously reported data^{19,20a} observed from the ^{13}C CP-MAS NMR spectroscopy.

Experimental Section

Unlabeled and ^2H -labeled Leu⁵- or Met⁵-enkephalins were synthesized by Fmoc chemistry on an Applied Biosystems 431A peptide synthesizer and purified by a reversed-phase high-pressure liquid chromatography (HPLC) after deprotection. Fmoc amino acids were purchased from Peptide Institute, Osaka, Japan. Fmoc phenylalanine of the deuterium-labeled ring (99% enriched) was synthesized by the reaction of 9-fluorenylmethyl *N*-succinimidyl carbonate (Fmoc-Osu, from Peptide Institute, Osaka, Japan) with $[^2\text{H}_5]$ phenylalanine (from CIL, Andover, MA) following the method of Paquet.²⁷ These peptides were crystallized from four kinds of solvent compositions, after neutralization of the saturated aqueous solution with 1 or 0.5 N KOH solution. Sample 1 (Leu⁵-enkephalin; trihydrate¹¹) was obtained by slow evaporation of the aqueous solution. Sample 2 (Leu⁵-enkephalin; monohydrate⁹) was crystallized by cooling the equimolecular solution ($\text{H}_2\text{O}/\text{methanol} = 1:1$) at 4 °C.

Sample 3 (Leu⁵-enkephalin; $2\text{H}_2\text{O}$, $2N,N$ -dimethylformamide; DMF, X (unspecified solvent)¹²) was obtained from the solution ($\text{H}_2\text{O}/\text{DMF} = 3:2$) by slow evaporation. Sample 4 (Met⁵-enkephalin; $5.5\text{H}_2\text{O}$ ¹³) was obtained by cooling the equimolecular mixture of ethanol and water at 4 °C. An amount of 60 mg of crystalline sample thus obtained was placed in 5 mm o.d. glass NMR sample tubes for ^2H NMR measurements and a zirconia rotor for ^{13}C CP-MAS measurements sealed with Araldyte (Ciba-Geigy) to prevent evaporation of the mother liquor.

^2H NMR spectra were recorded on a Chemagnetics CMX 400 NMR spectrometer at the ^2H resonance frequency of 61.4 MHz equipped with a wide line single resonance probe of a transverse solenoid coil for a 5 mm o.d. sample tube. ^2H NMR spectra were obtained using a quadrupole echo pulse sequence ($90^\circ - \tau - 90^\circ - \tau - \text{echo}$).^{28–30} Echo signals were collected using a sample rate of 500 ns/point with CYCLOPS phase cycling to avoid spectral distortion. Probe matching was carefully adjusted to give a symmetrical line shape. The delay times ($\tau = 30, 60, 90, \text{ or } 120 \mu\text{s}$) between the two pulses for the echo sequences and $30 \mu\text{s}$ were used for experiments for τ and temperature variations, respectively. The $\pi/2$ pulses were $2.0\text{--}3.0 \mu\text{s}$ and the recycle delay was 500 ms or 1 s. The time domain data were left-shifted to the echo maximum, and Lorentzian line broadening of 1 kHz was applied to the spectrum prior to Fourier transform. Spin-lattice relaxation times of deuterium nuclei (T_1^D) were measured by means of an inversion-recovery pulse sequence combined with the quadrupole echo sequence ($180^\circ - t - 90^\circ - \tau - 90^\circ - \tau - \text{echo}$). The pulse spacing τ was $30 \mu\text{s}$, and the spectra of six different delay times (t) were usually measured. The T_1^D values were evaluated by a nonlinear least-squares regression method for $M_0[1 - 2 \exp(-t/T_1)]$ using the six peak intensities. ^{13}C NMR spectra were recorded at the resonance frequency of 100.6 MHz using a double-resonance MAS probe for a 5 mm o.d. rotor. The method of CP-MAS combined with a TOSS (total suppression of spinning sidebands) pulse sequence³¹ was used. The $\pi/2$ pulse lengths for carbon and proton nuclei were $4.6\text{--}5.3 \mu\text{s}$, the contact time was 1 ms, and the recycle delay was 4 s. A ^1H decoupling field of 47–54 kHz was used, and the rotor spinning speed was controlled to 4000 ± 3 Hz. ^{13}C chemical shifts were referred to TMS through that of the carbonyl group (176.03 ppm) of crystalline glycine. ^2H NMR and ^{13}C CP-MAS spectra were recorded at 20–25 °C. Temperatures between 0 and –140 °C were controlled by using a cryostat based on liquid nitrogen. The probe temperatures were measured at the inlet temperature of the spinner assembly after waiting 10 min for equilibration. The numbers of acquisitions were varied from 1600 to 8000 for ^2H NMR experiments and from 300 to 1200 for ^{13}C CP-MAS NMR experiments, until the *S/N* ratio was more than 24 for ^2H NMR spectra and 26 for ^{13}C CP-MAS spectra. Spectral simulation for the deuterium NMR line shape was performed by using a two-site jump model between the C–D bond angle (2Θ) of 120° through the Internet site.³²

Results

Figure 1 (left) shows ^2H NMR spectra of a variety of $[^2\text{H}_5]$ -Phe⁴-labeled Leu⁵- or Met⁵-enkephalin crystals (1–4). The isotropic signals appearing at the center of the spectra are attributed to the bound solvent molecules of natural abundance in the polycrystalline enkephalins. It turned out from the spectral patterns that the phenyl rings undergo a 180° flip motion about the $C_\beta\text{--}C_\gamma$ axis, and their frequencies for samples 1–4 were estimated as 5.0×10^3 , 3.0×10^4 , 2.4×10^6 , and 1.0×10^4

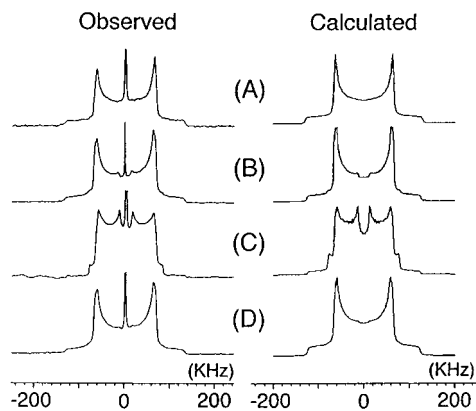


Figure 1. (A) Observed (left) and calculated (right) ^2H NMR spectra of Leu 5 -enkephalin crystallized from water (A), methanol/H $_2\text{O}$ (B), and DMF/H $_2\text{O}$ (C) and Met 5 -enkephalin crystallized from ethanol/H $_2\text{O}$ (D). The isotropic signal at 0 Hz is due to natural abundant solvent molecules. Lorentzian line broadening ($\text{lb} = 1000$ Hz) was applied prior to Fourier transformation. The 180° flip frequencies for the calculations are 5.0×10^3 (A), 3.0×10^4 (B), 2.4×10^6 (C), and 1.0×10^4 Hz (D). The asymmetry parameters, η , for the calculations are 0.02 (A), 0.05 (B), 0.05 (C), and 0.05 (D). $\tau = 30 \mu\text{s}$ was used for the calculations.

Hz, respectively, by comparing them with the simulated ^2H NMR line shapes for the aromatic rings as a function of the flipping rate. The best-fit spectra on the right-hand side of Figure 1 were obtained by adding the spectra of ortho and meta positions with the 180° flip frequencies mentioned above to that of the para position without flip motion ($\Theta = 0^\circ$) with the intensity ratio of 4:1. The resonances arising from the perpendicular components (highest doublet peaks) were broadened for all samples, which was due to the presence of the small asymmetry parameters, η , of 0.02 and 0.05 for sample 1 and samples 2–4, respectively.

Figure 2 illustrates the powder patterns obtained for the pulse intervals (τ) of 30 and 120 μs . A set of experimental and simulated spectra containing those of $\tau = 60$ and 90 μs are summarized in Figures 1S and 2S of the Supporting Information. As the interval was increased, the intensities of the spectra of samples 1 and 2 were decreased. For sample 4, only the perpendicular resonances were observed at the interval of 120 μs (Figure 2D). Spectral calculation was performed for the case of $\tau = 120 \mu\text{s}$ (as shown on the right-hand side of Figure 2). A large discrepancy was noticed for sample 4, although good agreement with the calculated spectra was seen for samples 1–3. To examine the effect of heterogeneity in the 180° flip frequencies of the phenyl ring, we have superimposed calculated line shapes for sample 4 for various correlation times weighted by a log-Gaussian distribution function, $P(\log \tau_c)$ with the standard deviation $\sigma = 1.0, 1.5,$ or 2.0 decades (Figure 3S of the Supporting Information). As demonstrated in spectrum 2 of Figure 2D ($\tau = 120 \mu\text{s}$) for $\sigma = 1.0$, the calculated line-shape is not consistent with the experimental one, and the observed discrepancy may be attributed to the presence of librations in addition to the 180° flip motion of the phenyl rings as is discussed later.

^2H spin–lattice relaxation times of the laboratory frame (T_1^D) were measured by using an inversion recovery method at room temperature (20–25 $^\circ\text{C}$). The values obtained at the three positions, parallel (α is the angle between the magnetic field vector \mathbf{B}_0 and the C– ^2H bond = 180°), perpendicular ($\alpha = 90^\circ$), and central ($\alpha = 54.7^\circ$) positions, were summarized in Table 1. We analyzed the correlation time (τ_c) for the case of a 180° flip motion of the phenyl rings by using eq 1, 24

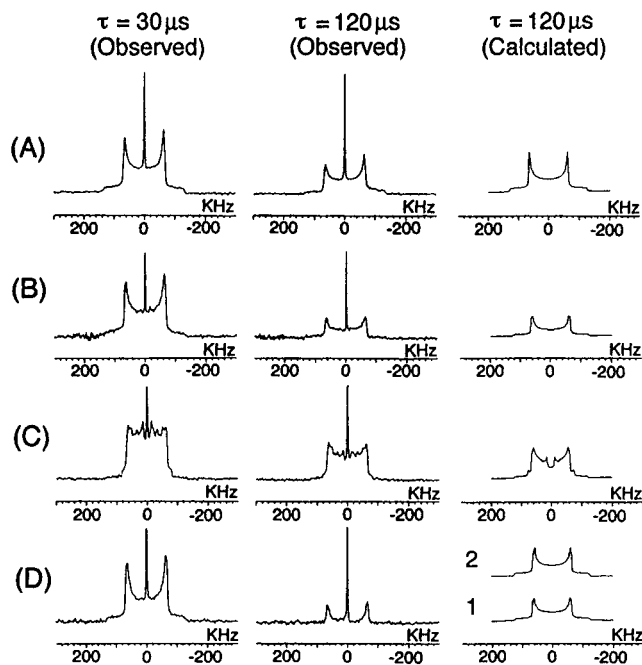


Figure 2. Stacked ^2H NMR spectra recorded at various pulse duration times (τ); (A)–(D) correspond to samples 1–4, respectively. Same parameters as Figure 1 were used for the simulation except for $\tau = 120 \mu\text{s}$. Spectra 1 and 2 of Figures 2D correspond to the simulated ^2H NMR spectra for $\sigma = 0$ and 1, respectively, taking into account of log-Gaussian distribution of correlation time for $\tau = 120 \mu\text{s}$.

TABLE 1: Experimental T_1^D Values (s) at Various Positions of ^2H Powder Patterns (A) and Calculated Values (B)

samples	$\alpha = 180^\circ$	$\alpha = 90^\circ$	$\alpha = 54.7^\circ$
1 (A)	0.41 (± 0.13)	0.56 (± 0.08)	0.72 (± 0.05)
(B)	0.35	0.45	0.42
2 (A)	0.09 (± 0.02)	0.16 (± 0.01)	0.20 (± 0.01)
(B)	0.13	0.16	0.14
3 (A)	0.065 (± 0.01)	0.12 (± 0.03)	0.099 (± 0.01)
(B)	0.076	0.098	0.082
4 (A)	0.18 (± 0.04)	0.19 (± 0.03)	0.22 (± 0.02)
(B)	0.15	0.20	0.19

$$\langle 1/T_1 \rangle = 1/5(\omega_Q/\omega_0)^2 \tau_c^{-1} \sin^2(2\Theta) \quad (1)$$

It was assumed that the 180° jump motion satisfied the slow-motional limit ($\omega_0 \tau_c \gg 1$), which was judged from the τ_c values determined by the line shape analysis. $\langle 1/T_1 \rangle$ means the averaged T_1^D value over all orientations and was evaluated experimentally by averaging out the T_1^D values at the three positions mentioned above for one powder pattern as summarized in Table 2. $\omega_0/2\pi = 61.4$ MHz is the Larmor frequency of deuterium, and $\omega_Q/2\pi$ is the deuterium quadrupole interaction determined from the peak splitting of the powder pattern. Θ is the angle between the C– ^2H bond axis and the flip axis, and 60° was used in the calculation. The correlation times (τ_c) obtained from the T_1^D values mentioned above and the correlation times of the 180° flip motion determined by comparing the observed line shape with the simulated one are also listed in Table 2. The frequencies of the motions obtained from the ^2H line shape analysis were 1–3 orders of magnitude smaller than those from the spin–lattice relaxation times.

^2H NMR spectra were recorded at various temperatures between 20 and -140 $^\circ\text{C}$ for these four samples as illustrated in Figure 3 for samples 3 and 4. Those for samples 1 and 2 are summarized in Figure 4S of the Supporting Information. It was found that the 180° flip motions of the phenyl rings became slower than 10^3 Hz at 0 $^\circ\text{C}$ for samples 1, 2, and 4 and -100

TABLE 2: T_1^D Values Measured by Inversion Recovery Method (s), Correlation Times (τ_c ; s and Hz) Determined from T_1^D Values, and the Frequencies of Flip-Flop Motions (Hz) Determined from Line Shape Analysis of Samples 1–4 at Ambient Temperature

samples	T_1^D (s)	correlation times	
		τ_c (s) [Hz]	flip-flop motion (Hz)
1	0.56	3.7×10^{-7} [2.7×10^6]	5.0×10^3
2	0.15	9.3×10^{-8} [1.1×10^7]	3.0×10^4
3	0.095	5.6×10^{-8} [1.8×10^7]	2.4×10^6
4	0.20	1.2×10^{-7} [8.3×10^6]	1.0×10^4

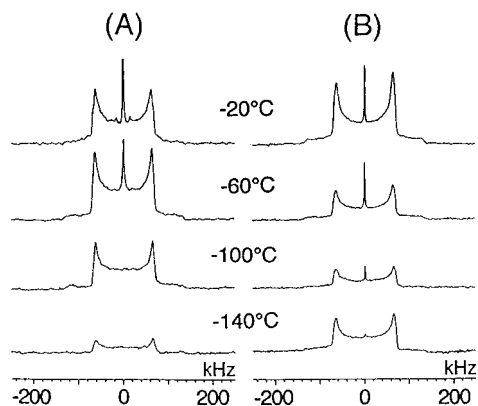


Figure 3. Stacked ^2H NMR spectra of samples 3 (A) and 4 (B) at various temperatures between -20 °C and -140 °C. The spectra were obtained by accumulating 6400 and 2000 transients, respectively.

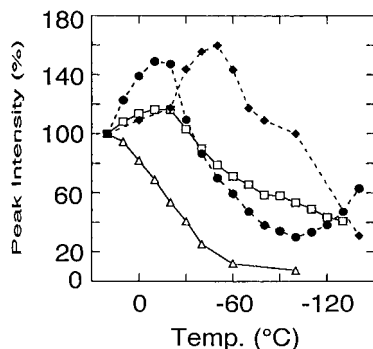


Figure 4. Plots of the percentages of the perpendicular peak intensities at various temperatures between 20 and -140 °C, with respect to the intensities at 20 °C as 100%, respectively: (Δ) sample 1; (\square) sample 2; (\blacklozenge) sample 3; (\bullet) sample 4. Pulse duration time was held as 1 s for sample 1 and 500 ms for samples 2–4.

°C for sample 3 because the line shapes did not show further changes below those temperatures. When the temperature was lowered, the intensities once increased up to -20 °C for samples 2 and 4 or -50 °C for sample 3, whereas that of sample 1 decreased gradually at lower temperature (Figure 4). Below those temperatures, the intensities for samples 2–4 decreased gradually. An exception was an increase of the intensity below -100 °C as seen for sample 4. The correlation times of the 180° flip motion were obtained at the temperatures 20, 10, 0, -20 , and -60 °C for sample 3 by the simulation of ^2H NMR spectra. These correlation times were plotted against the inverse of temperature (K) (Figure 5) and fitted to a simple activation law given by eq 2,^{24,33–35}

$$\tau_c = \tau_0 \exp(E/kT) \quad (2)$$

By using a linear least-squares regression method, the activation energy of $E = 37.5$ kJ/mol (8.96 kcal/mol) and $\tau_0 = 7.0 \times$

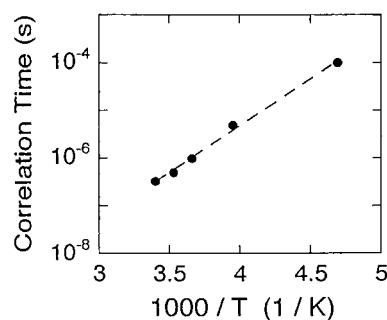


Figure 5. Arrhenius plot of the correlation times of the 180° flip motion (Hz) against the temperatures for sample 3.

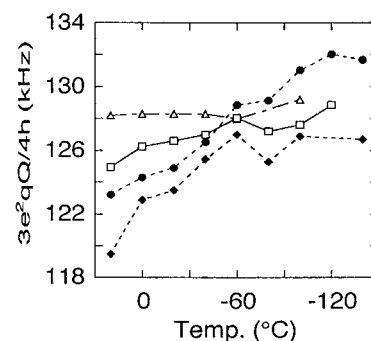


Figure 6. Plots of the quadrupolar coupling constants (Hz) against various temperatures between 20 and -140 °C. The plot style for samples 1–4 is the same as that in Figure 4.

10^{-14} s were obtained. The activation energy for samples 1, 2, and 4 were not obtained from the line shape analysis of ^2H NMR spectra because any spectral changes were noted below 0 °C.

As the temperature was lowered, the splittings (± 1.5 kHz) of the ^2H NMR spectra for samples 1–4 were gradually increased, and those observed at -100 °C were larger than those at ambient temperature by 1.0, 4.0, 4.7, and 7.8 kHz, respectively (Figure 6). This proves that rapid librations with a small amplitude which does not seriously perturb the ^2H spectral patterns also exist in the phenyl rings in addition to the 180° flip motions in the crystalline state. It is of interest to note that the quadrupole splittings for sample 4 monotonically increased even at -120 °C, whereas they became constant for samples 1–3. This fact indicates that the amplitude of the librations for sample 4 is the largest and does not cease even at temperatures as low as -120 °C.

^{13}C CP-MAS spectra of samples 1–4 were measured at several temperatures between room temperature (20–25 °C) and -140 °C. The stacked plots for samples 3 and 4 are shown in Figures 7 and 8, respectively. As observed in samples 1¹⁹ and 2,²⁰ the emerging new resonances, i.e., Tyr C_ϵ for sample 3 and Met COO^- for sample 4, or broadening of peaks were noticeable as the temperature was lowered. Recovery of the signal intensities from the interference with the proton decoupling frequency (47–54 kHz) exhibited at room temperature was successively observed for the aromatic resonances at lower temperatures for samples 1, 2, and 4. For sample 3, the peak intensities of Phe C_δ , C_ϵ , and C_ζ decreased from 25 to -40 °C and the intensities began to recover below -40 °C, whereas those of Tyr C_δ and C_ϵ recovered gradually below 0 °C. The recovery for sample 3 was different from those of the other three samples. The above-mentioned spectral changes turned out to be completely reversible (Figures 5S, 6S, and 7S for samples 2, 3, and 4, respectively, in the Supporting Information).¹⁹

The peak intensities of the solvent resonances at 0 Hz in the

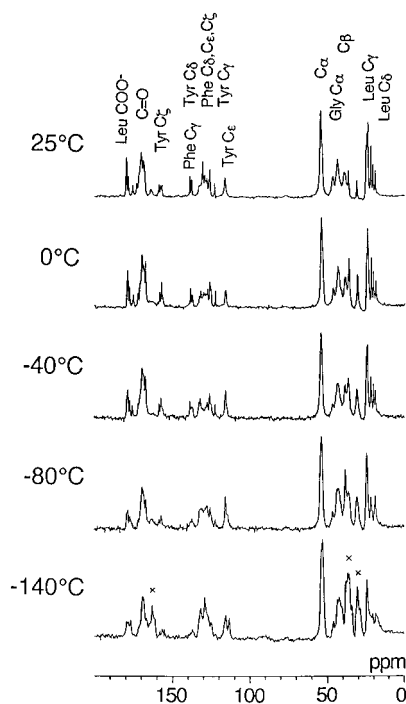


Figure 7. Stacked ^{13}C CP-MAS NMR spectra of sample 3 recorded at various temperatures between 25 and -120 °C. The peaks marked by \times are assigned to the methyl and carbonyl signals of DMF.

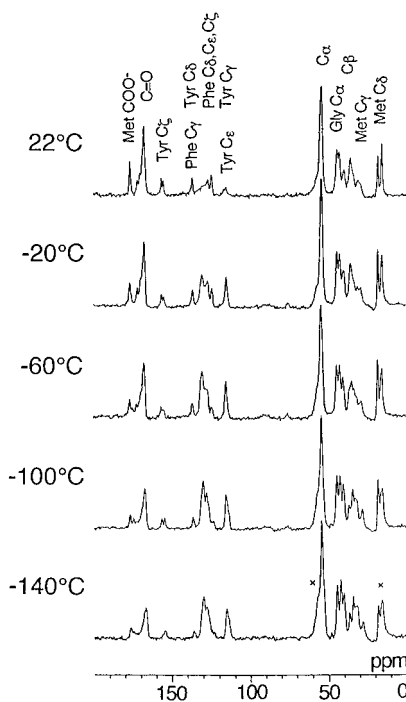


Figure 8. Stacked ^{13}C CP-MAS NMR spectra of sample 4 recorded at various temperatures between 22 and -140 °C. The peaks marked by \times are assigned to the methyl and methylene signals of ethanol.

deuterium NMR spectra, which are attributed to naturally abundant deuterium nuclei in the solvent molecules undergoing fast isotropic motion, were decreased as the temperature was lowered (Figure 9). The freezing points of neat or mixed solvents such as water, methanol/water (1:1), DMF/water (1:1), and ethanol/water (1:1) used for crystallization of samples 1–4, are 0, -54.5 , -49.4 , and -37.6 °C, respectively, and actually their intensities were decreased gradually and stepwise not only at around these temperatures but also at the other temperatures by two steps for samples 1–3 and three steps for sample 4.

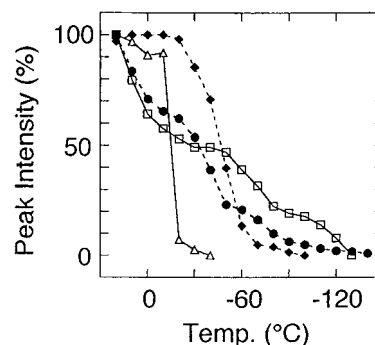


Figure 9. Plots of the percentages of the peak intensities at 0 Hz due to the natural abundant solvent molecules, at various temperatures between 20 and -140 °C, with reference to their intensities at 20 °C as 100%, respectively. The plot style for samples 1–4 is the same as that in Figure 4.

Finally, the resonances completely disappeared at -40 , -130 , and -100 °C, for sample 1–3, respectively. Surprisingly, they did not completely disappear even at -140 °C for sample 4.

Discussion

Characterization of the Phenyl Ring Motion in the Crystals. First we characterized the 180° flip motion of the phenyl rings in enkephalin crystals by inspecting the ^{13}C CP-MAS (Figures 7 and 8)^{19,20a} and ^2H NMR spectra (Figure 3) at various temperatures. From the ^{13}C CP-MAS spectra it turned out that the phenyl rings have a motion with the frequency close to the proton decoupling (c.a. 50 kHz) at ambient temperature.^{19,20a} More specific information on the 180° flip motion of the phenyl rings at ambient temperature was determined from the simulated ^2H powder patterns as summarized in Table 2. It is evident that the frequencies of the phenyl ring motions for samples 2 and 4 were close to the proton decoupling frequency, whereas that of sample 1 was lower and that of sample 3 was higher than the decoupling frequency. It was therefore apparent for sample 3 that the peak intensities of Phe C_δ and C_ϵ were decreased between ambient temperature and -40 °C in the ^{13}C NMR spectra because of the interference between the decoupling frequencies and the 180° flip motion of phenyl rings. As the temperature was lowered, the ^2H NMR peak intensities of each sample were also varied as shown in Figure 4. The recovery of the peak intensities at room temperature to those at -20 °C for samples 2 and 4 or to -60 °C for sample 3 was observed because of the recovery from the loss of quadrupolar echo refocusing efficiency.³⁶ The reduced intensities for samples 2 and 4 at temperatures below -20 °C and sample 3 below -60 °C can be explained by the fact that the deuterium spin–lattice relaxation times were longer than the pulse duration time (500 ms). As for sample 1, the intensities were monotonically decreased below ambient temperature because the correlation time of the 180° flip motion was already long, showing that the interference in ^2H NMR spectra was reduced and that the saturation of magnetization occurred even at ambient temperature because of the long spin–lattice relaxation times.

Second, we found that fast librations with a small amplitude exists in the phenyl rings of enkephalin crystals besides the 180° flip motion at room temperature,^{22–24} because the quadrupolar coupling constants were averaged by 1–7.8 kHz at ambient temperature and deviation was observed between the correlation times evaluated from the ^2H NMR line shape and the spin–lattice relaxation times. Furthermore, this motion mainly contributes to the spin–lattice relaxation process because the correlation time is the same order as the deuterium Larmor

frequency. If they have only a 180° flip motion, the T_1^D values of the phenyl rings for samples **1–4** are estimated as 306.5, 53.7, 0.70, and 165.5 s, respectively, using eq 1 with the correlation times obtained from the line shape analyses. Because these values are 1–3 orders of magnitude longer than those obtained from the T_1^D measurements, it is also strongly suggested that there exists librations in addition to the 180° flip motion.

The change of the quadrupolar coupling constant at lower temperature for sample **4** was, however, the largest among the four samples. It is therefore suggested that the amplitude of the librations for sample **4** is the largest. This property is supported by the fact that the peak intensity of sample **4** increased below –100 °C after once it decreased gradually by the saturation of magnetization. The ratio of recovery of the intensity from –100 to –140 °C (~2.5) was larger than that obtained from the Boltzmann distribution ratio (~1.3). Thus, the increased intensity for sample **4** is regarded as the recovery from the interference of the fast librations with relatively larger amplitude and quadrupolar echo refocusing efficiency. Alternatively, it is likely that freezing of solvent motions changed the molecular packing in the crystal and allowed the motion of phenyl rings. This happened for the two phenyl rings of Gly-Phe-Phe in insulin fragments in crystals; the flipping motion was induced by the removal of water molecules.²⁵ The relatively large-amplitude librations in the case of sample **4** may also cause the significant distortion of the powder pattern obtained for a long pulse spacing in the quadrupole echo pulse sequence as shown in Figure 2. We have also considered the distribution of correlation times in the 180° flip. It turned out, however, that our result (spectrum 2 of Figure 2D for $\tau = 120 \mu\text{s}$ and Figure 3S of the Supporting Information) is not in good agreement with the experimental finding. Therefore, we concluded that the existence of the large-amplitude motion rather than the distribution of correlation times causes substantial deviation from the spectrum due to a single 180° flip motion.³⁷

When the ^2H relaxation times were measured in this study, a small anisotropy for the T_1^D values was observed for all samples (Table 1 (A)). The anisotropy for the T_1^D values were calculated using eq 3²⁴ by assuming that the C– ^2H bond axis of the phenyl ring undergoes a 180° flip²⁴ about the $\text{C}_\beta\text{--C}_\gamma$ axis with the angle of 2Θ and θ being the angle between the static field \mathbf{B}_0 and the flip axis as summarized in Table 1 (B).

$$1/T_1 = 1/8 \omega_Q^2 \sin^2(2\Theta) \{ [\cos^2 \theta + \cos^2(2\theta)] g(\omega_0, \tau_c) + [4 \sin^2 \theta + \sin^2(2\theta)] g(2\omega_0, \tau_c) \} \\ g(\omega_0, \tau_c) = \tau_c / (1 + \omega_0^2 \tau_c^2) \quad (3)$$

τ_c is the correlation time of the 180° flip motion, although the values are obtained from the averaged T_1^D values as listed in Table 2. \mathbf{B}_0 is the magnetic field vector and is parallel to the C– ^2H bond axis [$\alpha = 180^\circ$; $(\Theta, \theta) = (60^\circ, 60^\circ)$], perpendicular to the C– ^2H bond axis [$\alpha = 90^\circ$; $(\Theta, \theta) = (60^\circ, 30^\circ)$], and making an angle of 54.7° between \mathbf{B}_0 and the C– ^2H bond axis [$\alpha = 54.7^\circ$; $(\Theta, \theta) = (60^\circ, 5.3^\circ)$]. It is shown that the largest T_1^D values of the calculated ones are those of the resonances at $\alpha = 90^\circ$. In contrast, the values obtained from the T_1^D measurements showed that the maximum values were obtained at $\alpha = 54.7^\circ$, except for sample **3**. Because a large discrepancy was obtained between the experimentally obtained and the calculated T_1^D anisotropy, it also supports the existence of motions other than the 180° flip of phenyl rings.

^{13}C spin–lattice relaxation times of these phenyl rings were measured in our previous paper.^{20a} The T_1^C values for the Phe

C_δ , C_ϵ , and C_ζ carbons were almost the same despite the presence of the 180° flip motion which does not affect the relaxation time for the C_ζ carbon. This fact indicates that the fast motion besides the 180° flip motion is not only due to the motion around the $\text{C}_\beta\text{--C}_\gamma$ bond axis but also to that of the whole rings. As for the backbone of enkephalin molecules in the crystalline states, shorter spin–spin relaxation times (T_2) of carbonyl carbons³⁸ and shorter spin–lattice relaxation times (T_1^C) of C_α carbons of glycine for sample **1**^{20a} have been reported, indicating the existence of a backbone motion. This kind of motion may result in the librations of the phenyl ring.

Phenyl Ring Dynamics in View of Molecular Packing. It is of interest to correlate the above molecular motions with the manner of molecular packing in the crystals. The conformation was determined to be a double β -bend structure for sample **1**¹¹ and an extended structure for samples **3** and **4** by X-ray diffraction studies.^{12,13}

The most restricted motion at the phenyl rings among the four crystals was observed in this ^2H NMR study in sample **1**. This crystal has been characterized as a double β -bend structure which is stabilized by the two intramolecular hydrogen bonds.¹¹ This rather tight conformation causes the orthogonal close contact of the Tyr and Phe residues. Two Tyr¹ C_δ to Phe⁴ C_γ and C_δ distances were estimated as 2.67 and 2.70 Å, respectively,¹¹ from the structure determined by X-ray diffraction. These relatively short distances permit the phenylalanine side chains to interact with tyrosine side chains by $\pi\text{--}\pi$ interactions. Provided that the phenyl rings as an *address* site had an interaction with an aromatic side chain of an opioid receptor protein,^{16–18} the motion would be restricted, as is observed in sample **1**. This strong restriction of the 180° flip motion of the phenyl ring has also been observed in the Gly-Phe-Phe crystals.²⁵ In this crystal, two phenyl rings are located very close to each other by the strong hydrophobic interaction which results in very rigid phenyl rings in the presence of hydrated water. As for sample **1**, it is of interest to notice that enkephalin molecules are in a state of a chemical exchange between two kinds of conformations as shown by measuring the ^{15}N NMR resonances of amide nitrogen at ambient temperature.^{20a} As a consequence, the peptide backbone undergoes a motion of the frequency of $> 10^2 \text{ Hz}$. This chemical exchange proved that the backbone of enkephalin molecule is fairly flexible despite the rigidity of the phenyl rings for sample **1**.

The phenyl ring of sample **3** exhibits a 180° flip motion faster than that of sample **4**, although the two samples were classified as the same extended structures, antiparallel β -sheets connected by hydrogen bonds between molecules, by X-ray diffraction studies.^{11,12} Both for samples **3** and **4**, X-ray diffraction studies have revealed that the antiparallel β -sheet is roughly parallel to the crystallographic *ac* plane with the amino acid side chains oriented alternately above and below the plane. Thus, tyrosine and phenylalanine side chains are located above and below the backbone plane. The plates are stacked along the crystallographic *b* direction with the spacing of $b/2$, i.e., 12 and 9 Å for samples **3** and **4**, respectively. It is reasonable to consider that the longer spacing between the plates permits the phenyl ring to be more flexible. This is because the phenyl ring of sample **3** is more flexible than that of sample **4**.

An activation energy for the 180° flip motion of the phenyl ring was measured for sample **3**. The energy was smaller than those found for crystalline *p*-fluoro-D,L-phenylalanine below 100 °C (20 kcal/mol) and above 100 °C (11.3 kcal/mol),²⁴ tyrosyl ring in Leu⁵-enkephalin crystal (9.8 kcal/mol),²⁶ or phenyl ring in bacteriorhodopsin (12 kcal/mol).³⁹ Compared with these

results, the environment of the phenyl rings in sample **3** is shown to be highly flexible.

On the other hand, the initially proposed β -bend structure for sample **2** determined by the X-ray diffraction study^{9a} was latter withdrawn because further refinement of this form was unsuccessful.^{9b} Although it was determined recently by ¹³C REDOR NMR spectroscopy^{20b} that the enkephalin molecule in sample **2** is a bend form with quite different torsion angles from that previously reported,^{9a} the molecular packing around the phenyl ring in the crystals was not known. As estimated from these ²H NMR studies, however, the phenyl ring in sample **2** is not packed tightly in space with the other ones of the same (tyrosyl ring) or other molecules compared with those of samples **1** and **4** mentioned above.

Role of Solvent Molecules in the Conformation of Enkephalin Crystals. We have ascribed the observed isotropic signals at 0 Hz in the ²H NMR spectra of the enkephalin crystals to the natural abundant deuterium from solvents for crystallization and solvated molecules in the crystals. Alternatively, it may be worthwhile to consider the possibility of the phenyl rings undergoing fast continuous isotropic rotational diffusion.²³ The process of mobile phenyl rings in the crystals was ruled out because the atomic positions of the phenyl rings in the crystals have been determined with comparable thermal factors with those of other atoms by X-ray diffraction studies.^{9,11–13} Then, we consider that the isotropic signals consist of the natural abundant deuterium of solvents and the labeled deuterium of a little amount of free [²H₅]Phe⁴-enkephalin in the solvent.

The T_1^D values of these solvent molecules for sample **1–4** at ambient temperature were 0.030, 0.026, 0.005, and 0.037 s, respectively, which were much shorter than those of the phenyl rings, indicating that the signals are ascribed to solvent molecules with a rapid tumbling motion. It is interesting to point out that the intensities were decreased not only around the freezing points of neat or mixed solvent (0, –54.5, –49.4, and –37.6 °C for water, methanol/water, DMF/water, and ethanol/water, respectively, when they were mixed as the ratio 1:1) but also at the other temperatures by two steps for samples **1–3** and three steps for sample **4**. This decrease of the peak intensities by several steps indicates that the several kinds of mobile solvent molecules are bound in these crystals. The motion of them was frozen gradually at different temperatures along their hydrogen bonds networks among the solvent molecules. Furthermore, it was noticed that ¹³C CP-MAS resonances of the organic solvent appeared at lower temperature than the freezing points of mixed solvents,^{20a} whereas they did not appear at a higher temperature than those. Thus, the steep decrease of the isotropic ²H NMR signals due to the freezing of solvent motions can be classified as three types as follows: (1) freezing of motions in water molecules at around 0 to –20 °C; (2) freezing of motions in mixed solvents at around –30 to –70 °C for samples **2–4**; (3) freezing of motions in organic solvents at around –60 to –140 °C for samples **2–4** that are accompanied with the appearance of the ¹³C CP-MAS signals.

It is worthwhile to relate the ¹³C CP-MAS resonances of enkephalin molecules in the crystals to the isotropic ²H NMR resonances to reveal the role of solvent molecules in stabilizing the conformation of enkephalin molecules. This can be done because the ¹³C chemical shifts reflect the conformation of molecules and isotropic ²H NMR resonances indicate the manner of mobile solvent molecules at various temperatures. Actually, it was found that the changes of ¹³C CP-MAS NMR spectra occurred corresponding to the decrease of the isotropic intensities in the ²H NMR spectra. As for the case of sample **4**, the

¹³C CP-MAS resonances for the aromatic, carbonyl, and carboxyl carbons were broadened and the peak intensities of aromatic resonances began to recover at –20 °C when the isotropic peak intensity in ²H NMR spectra finished the steep decreasing as a first step (Figures 8 and 9). After the second step of the decrease of the ²H peak intensity from –30 to –50 °C which may occur by the freezing of mixed solvent molecules (–37.6 °C), a new carboxyl signal in ¹³C CP-MAS spectra began to appear in the lower frequency side of the carboxyl signal observed at ambient temperature and the aromatic resonances recovered their intensities. These results suggest that the mixed solvent molecules which are not strongly bound to crystals play an important role in stabilizing the conformation of enkephalin molecules in the crystals. It is therefore appropriate to consider that the carboxyl groups which form hydrogen bonds with a few kinds of solvent molecules change the manner of hydrogen bond networks as the solvent freezes. In the third and fourth steps of the decrease of the isotropic ²H NMR peak, the peptide backbone also seemed to change its torsion angles because the splitting of two Gly C α signals spread from 1.4 to 2.2 ppm besides the change of line shape in the carbonyl resonances. On the other hand, the dynamics of aromatic rings is not apparently influenced by the freezing of solvent molecules for samples **1**, **2**, and **4**. This is judged from the observation that the splitting of the perpendicular component of the ²H NMR pattern of the phenyl ring increased monotonically rather than stepwise as the temperature decreased. At very low temperatures, there was a shallow basin at –60 °C in a plot of the quadrupolar splittings against temperature for sample **3** (Figure 4). This may indicate an exception that the freezing of motions in organic solvent causes a change of the phenyl ring dynamics. It is therefore emphasized that the conformational change rather than the change of phenyl ring dynamics is caused by the freezing motions of solvent molecules. In general, we believe that isotropic ²H NMR signals allow one to reveal answers to the question of how the solvent molecules stabilize the conformation of molecules in the crystals.

Conclusion

It has been proven that the phenyl rings in enkephalin molecules in a variety of crystals undergo 180° flip motions with different frequencies. These differences can be explained in terms of the different manner of molecular packing in the crystals. In addition to the 180° flip motion, small-amplitude librations were detected in enkephalin in the crystalline states. These librations were responsible for the mechanism of the spin–lattice relaxation process for the ring deuterons. It is also found that several kinds of solvent molecules are present in the crystals and that these freeze at different temperatures. Some of the solvents induce a local conformational change of enkephalin molecules in the crystals. It is therefore concluded that the flexibility of the backbone in enkephalin molecules is strongly influenced by the state of the solvent molecules.

Acknowledgment. We are grateful to Drs. H. W. Spiess and V. Macho of Max-Planck-Institut für Polymerforschung for giving us the opportunity to perform spectral simulation at Mainz and for their technical advice. This work was supported, in part, by Grants-in-Aid for Scientific Research from the Ministry of Education, Science, Culture and Sports of Japan (09558094, 09640612, 0645466, 09261233).

Supporting Information Available: Seven figures showing the experimental (Figure 1S) and simulated ²H NMR spectra

(Figure 2S) at $\tau = 30, 60, 90,$ and $120 \mu\text{s}$ for the samples 1–4, superposition of simulated ^2H NMR spectra for various correlation times weighted by a log-Gaussian distribution function with standard deviation $\sigma = 1-2$ (Figure 3S), ^2H NMR spectra at lower temperature for samples 1 and 2 (Figure 4S), ^{13}C CP-MAS spectra at 20°C before and after the temperatures were lowered (Figures 5S, 6S and 7S for samples 2, 3, and 4, respectively). This material is available free of charge via the Internet at <http://pubs.acs.org>.

References and Notes

- (1) Hughes, J.; Smith, T. W.; Kosterlitz, H. W.; Fothergill, L. A.; Morgan, B. A.; Morris, H. R. *Nature* **1975**, *258*, 577.
- (2) Chavkin, C.; Goldstein, A. *Proc. Natl. Acad. Sci. U.S.A.* **1981**, *78*, 6543.
- (3) Wolozin, B. L.; Pasternak, G. W. *Proc. Natl. Acad. Sci. U.S.A.* **1981**, *78*, 6181.
- (4) Schiller, P. W. In *The Peptides, Analysis, Synthesis, Biology*; Udenfriend, S., Meienhofer, J., Eds.; Academic Press: Orlando, 1984; Vol. 6, p 269.
- (5) Higashijima, T.; Kobayashi, J.; Nagai, U.; Miyazawa, T. *Eur. J. Biochem.* **1979**, *97*, 43.
- (6) Graham, W. H.; Carter, E. S., II; Hicks, R. P. *Biopolymers* **1992**, *32*, 1755.
- (7) Marion, D.; Garbay-Jauregui, C.; Roques, B. P. *J. Magn. Reson.* **1983**, *53*, 199.
- (8) Stimson, E. R.; Meinwald, Y. C.; Scheraga, H. A. *Biochemistry* **1979**, *18*, 1661.
- (9) (a) Smith, G. D.; Griffin, J. F. *Science* **1977**, *199*, 1214. (b) Blundell, T. L.; Hearn, L.; Tickle, I. J.; Palmer, R. A.; Morgan, B. A.; Smith, G. D.; Griffin, J. F. *Science* **1979**, *205*, 220.
- (10) Ishida, T.; Kenmotsu, M.; Mino, Y.; Inoue, M.; Fujiwara, T.; Tomita, K.; Kimura, T.; Sakakibara, S. *Biochem. J.* **1984**, *218*, 677.
- (11) (a) Aubry, A.; Birlirakis, N.; Sakarellos-Daitsiotis, M.; Sakarellos, C.; Marraud, M. *J. Chem. Soc., Chem. Commun.* **1988**, 963. (b) Aubry, A.; Birlirakis, N.; Sakarellos-Daitsiotis, M.; Sakarellos, C.; Marraud, M. *Biopolymers* **1989**, *28*, 27. (c) Wiest, R.; Pichon-Pesme, V.; Bénard, M.; Lecomte, C. *J. Phys. Chem.* **1994**, *98*, 1351.
- (12) (a) Camerman, A.; Mastropaolo, D.; Karle, I. L.; Karle, J.; Camerman, N. *Nature* **1983**, *306*, 447. (b) Karle, I. L.; Karle, J.; Mastropaolo, D.; Camerman, A.; Camerman, N. *Acta Crystallogr.* **1983**, *B39*, 625.
- (13) Mastropaolo, D.; Camerman, A.; Camerman, N. *Biochem. Biophys. Res. Commun.* **1986**, *134*, 698.
- (14) Griffin, J. F.; Langs, D. A.; Smith, G. D.; Blundell, T. L.; Tickle, I. J.; Bedarkar, S. *Proc. Natl. Acad. Sci. U.S.A.* **1986**, *83*, 3272.
- (15) Doi, M.; Tanaka, M.; Ishida, T.; Inoue, M.; Fujiwara, T.; Tomita, K.; Kimura, T.; Sakakibara, S.; Sheldrick, G. M. *J. Biochem.* **1987**, *101*, 485.
- (16) Portoghese, P. S.; Sultana, M.; Nagase, H.; Takemori, A. E. *Recent Advances in Receptor Chemistry*; Elsevier Science Publishers: Amsterdam, 1988; pp 307–317.
- (17) Portoghese, P. S. *Trends Pharmacol. Sci.* **1989**, *10*, 230.
- (18) Portoghese, P. S. In *Trends in Medicinal Chemistry*; Mutschler, E., Winterfeldt, E., Eds.; VCH Verlagsgesellschaft: Weinheim, 1987; pp 327–336.
- (19) Naito, A.; Kamihira, M.; Tuzi, S.; Saitô, H. *J. Phys. Chem.* **1995**, *99*, 12041.
- (20) (a) Kamihira, M.; Naito, A.; Nishimura, K.; Tuzi, S.; Saitô, H. *J. Phys. Chem.* **1998**, *102*, 2826. (b) Nishimura, K.; Naito, A.; Tuzi, S.; Saitô, H.; Hashimoto, C.; Aida, M. *J. Phys. Chem.* **1998**, *102*, 7476.
- (21) (a) Wittebort, R. J.; Olejniczak, E. T.; Griffin, R. G. *J. Chem. Phys.* **1987**, *86*, 5411. (b) Schmidt-Rohr, K.; Spiess, H. W. *Multidimensional Solid-State NMR and Polymers*; Academic Press: London, 1994.
- (22) Gall, C. M.; Diverdi, J. A.; Opella, S. J. *J. Am. Chem. Soc.* **1981**, *103*, 5039.
- (23) Kinsey, R. A.; Kintanar, A.; Oldfield, E. *J. Biol. Chem.* **1981**, *256*, 9028.
- (24) Hiyama, Y.; Silverton, J. V.; Torchia, D. A.; Gerig, J. T.; Hammond, S. J. *J. Am. Chem. Soc.* **1986**, *108*, 2715.
- (25) Naito, A.; Iizuka, T.; Tuzi, S.; Price, W. S.; Hayamizu, K.; Saitô, H. *J. Mol. Struct.* **1995**, *355*, 55.
- (26) Rice, D. M.; Wittebort, R. J.; Griffin, R. G.; Meirovitch, E.; Stimson, E. R.; Meinwald, Y. C.; Freed, J. H.; Scheraga, H. A. *J. Am. Chem. Soc.* **1981**, *103*, 7707.
- (27) Paquet, A. *Can. J. Chem.* **1982**, *60*, 976.
- (28) Davis, J. H.; Jeffery, K. R.; Bloom, M.; Valic, M. I.; Higgs, T. P. *Chem. Phys. Lett.* **1976**, *42*, 390.
- (29) Bloom, M.; Davis, J. H.; Valic, M. I. *Can. J. Phys.* **1980**, *58*, 1510.
- (30) Spiess, H. W. *J. Chem. Phys.* **1980**, *72*, 6755.
- (31) Dixon, W. T. *J. Chem. Phys.* **1982**, *77*, 1800.
- (32) (a) Schmidt-Rohr, K.; Spiess, H. W. *Multidimensional Solid-State NMR and Polymers*; Academic Press: London, 1994; pp 32–35. (b) Lirvinov, V. M.; Macho, V.; Spiess, H. W. *Acta Polym.* **1997**, *48*, 471. Calculation was performed at Max-Planck-Institut für Polymerforschung, Mainz through <http://www.mpip-mainz.mpg.de/weblab/weblab.html>.
- (33) Andrew, E. R.; Hinshaw, W. S.; Hutchins, M. G.; Sjöblom, R. O. *I. Mol. Phys.* **1976**, *31*, 1479.
- (34) Andrew, E. R.; Hinshaw, W. S.; Hutchins, M. G.; Sjöblom, R. O. *I. Mol. Phys.* **1976**, *32*, 795.
- (35) Andrew, E. R.; Hinshaw, W. S.; Hutchins, M. G.; Sjöblom, R. O. *I. Mol. Phys.* **1977**, *34*, 1695.
- (36) Schadt, R. J.; Cain, E. J.; English, A. D. *J. Phys. Chem.* **1993**, *97*, 8387.
- (37) Greenfield, M. S.; Ronemus, A. D.; Vold, R. L.; Vold, R. R.; Ellis, P. D.; Raidy, T. E. *J. Magn. Reson.* **1987**, *72*, 89.
- (38) Naito, A.; Fukutani, A.; Uitdehaag, M.; Tuzi, S.; Saitô, H. *J. Mol. Struct.* **1998**, *441*, 231.
- (39) Rice, D. M.; Meinwald, Y. C.; Scheraga, H. A.; Griffin, R. G. *J. Am. Chem. Soc.* **1987**, *109*, 1636.